Optik - International Journal for Light and Electron Optics 226 (2021) 165806

Contents lists available at ScienceDirect

Optik

journal homepage: www.elsevier.com/locate/ijleo

Original research article

Parameter calibration of 6-degree-of-freedom parallel mechanism based on orthogonal displacement measuring system

Yang Liwei *, Fan Yanchao, Chai Fangmao, Pang Xinyuan, Dong deyi

Changchun Institute of Optics, Fine Mechanics and Physics, Chinese Academy of Sciences, Changchun, Jilin, 130033, China

ARTICLE INFO

Keywords:
6-DOF parallel mechanism
Orthogonal displacement measuring (ODM) system
Parameter identification
Optimization algorithm
OASIS software

ABSTRACT

Aiming at simplifying the parameter calibration process of the 6 degree-of-freedom(6-DOF) parallel mechanism, improving the calibration efficiency, and reducing the calibration cost, this paper proposes a pose measurement device and method based on the Orthogonal Displacement Measurement (ODM) system. First, the pose calculation method of the proposed device is studied, and its forward and inverse kinematics solutions are solved using spatial analytic geometry method; second, an error model for the combination of the parallel mechanism and the ODM system is constructed using the infinitesimal displacement synthesis method; third, based on the proposed error model, a mathematical model is constructed for the optimization problem of the parameter error identification of the combination, wherein the minimization of the sum of squares of *in*, the indicating value displayed by the sensor, is taken as the objective function, and the structural parameter errors of the combination are taken as the design variables; at last, the ODM system is used to measure the pose of the 6-DOF parallel mechanism, and the OASIS software is adopted to directly find out the optimal solutions of the parameter errors and compensate them to the parallel mechanism control system, so as to complete the parameter calibration of the parallel mechanism. The comparison result of the pose errors before and after the calibration shows that, the maximum position error has been reduced by 69 %–94 %, and the maximum posture error has been reduced by 87 %–97 %. Using ODM system to calibrate the parameters of the parallel mechanism can not only effectively improve the positioning accuracy of the parallel mechanism, but also simplify the calibration work, improve the calibration efficiency, and reduce the calibration cost.

1. Introduction

The 6-DOF parallel mechanism is widely used in the fields of optical components fine tuning, and ultra-precision machining due to its advantages of high precision, high rigidity, and no cumulative error, etc. [1].

Due to machining and assembly errors, the actual structural parameters of the 6-DOF parallel mechanism are somewhat different from the theoretical values, resulting in kinematic model inaccuracy. Because of the existence of structural parameter errors, when the 6-DOF parallel mechanism performs movements according to the instructions, there're certain deviations between the actual pose and the theoretical ones. Using high-precision machine tools to process the structural components of the parallel mechanism can reduce the machining errors, but its cost is very high; in such case, using parameter calibration to compensate the errors is a low-cost and effective

* Corresponding author.
E-mail address: 13604415684@126.com (Y. Liwei).

https://doi.org/10.1016/j.ijleo.2020.165806
Received 18 July 2020; Accepted 13 October 2020
Available online 6 November 2020
0030-4026/

method [2,3].

Generally speaking, the calibration of parallel mechanism includes the following three steps: error modeling, pose measurement, and parameter identification. Wherein, the pose measurement of the end effector of the parallel mechanism is the key link of calibration process; during calibration, according to the measurement output, the calibration can be divided into two types: self-calibration and external calibration [4]. The self-calibration method does not require external measurement equipment, it uses the redundant information derived from the moving platform to identify its geometric parameters; in the calibration process, this method has to solve the forward solutions of the calibration model, and it cannot obtain all information of the end pose, thereby its accuracy improvement is limited by certain restrictions. The external calibration method is also called open-loop calibration, which uses external measurement equipment to acquire the pose information of the moving platform, and identify the geometric parameters of the platform accordingly. Now external calibration is still the main method for the calibration of parallel mechanisms, and commonly used external measurement equipment includes: coordinate measuring machine (CMM) [4], measuring arm [5], laser tracker [6] and other devices. Although these devices generally have high accuracy and wide adaptability, they are expensive to manufacture and there're two problems with them during application: first, the measuring equipment needs to be finely adjusted before measurement, which would take a long time, and the calibration efficiency is relatively low; second, some measuring equipment (such as CMM) has a high requirement on the operators and the operating environment, so its application is not that convenient. Based on the above reasons, the above-mentioned pose measurement solutions need to be further improved.

Aiming at the problems existing in the measurement process of the pose of the 6-DOF parallel mechanism, this paper proposes a simple and efficient 6-DOF parallel mechanism parameter calibration device and method, in the hopes of achieving the purpose of reducing calibration cost, simplifying calibration process, and improving calibration efficiency. This study has a very important guiding significance for the parameter calibration of parallel mechanisms.

2. Forward and inverse solutions of the ODM system

2.1. Composition of ODM system

The traditional pose measurement method is simple to operate and has a wide application range, however, since the coordinates of the reference point cannot be obtained directly from measurement, but from the fitting of multiple sampling points, its requirement on data volume is relatively large, and its calibration efficiency is low. With a simplest case, the fitting of spherical surface as an example, at least 5 points are required to fit the coordinates of a reference point, and at least 3 points are required to solve the pose, that is to say, for each end pose, at least 15 points need to be measured to solve its corresponding actual pose, obviously, this method is both time and energy consuming.

Inspired by the laser 6-dimensional measurement system [7,8], this study attempts to construct a contact-type orthogonal displacement measuring system (hereinafter referred to as the ODM system) to carry out the measurement and calculation of the pose of moving platform of parallel mechanism. Fig. 1 shows a schematic diagram of the ODM system, which includes the reference block to be measured (namely the target reference block), and the displacement sensors, etc. Wherein the target reference block is fixed on the moving platform, several displacement sensors are placed in the three orthogonal directions of the target reference block, all displacement sensors are fixed on the sensor stand, and there's no relative movement between the sensor stand and the fixed platform; under the action of the elastic force, the displacement sensor is always in contact with the target reference block. The working principle is as follows: the moving platform performs 6-dimensional movements according to the instructions of the controller, the target

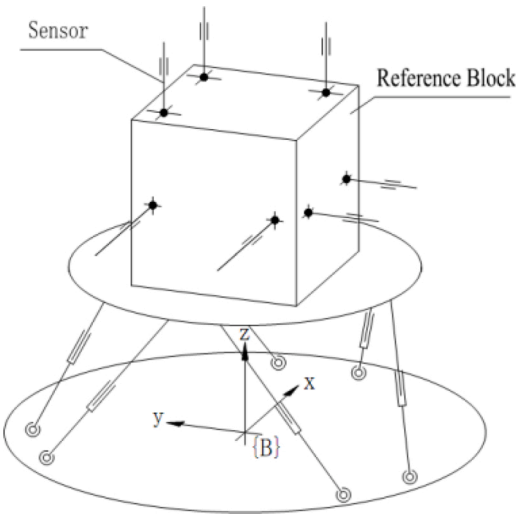

Fig. 1. diagram of the ODM system.

reference block moves with it accordingly, and the displacement sensors perform 1-dimensional stretching out and drawing back movements; then the indicating values of the displacement sensors are recorded, then with certain solving method, the pose of the moving platform relative to fixed platform are calculated.

It can be seen from the figure that the ODM system can be regarded as a set of mechanisms, the driving part is the end effector of the parallel mechanism, and the driven part is the displacement sensor. The 6-dimensional movement of the effector produces the 1-dimensional linear movement of the displacement sensor, and the solving process of the pose of the end effector is the process of the kinematic analysis of the ODM system.

Just like the parallel mechanism, the kinematic analysis of the ODM system also has two basic questions, namely the forward solution and the inverse solution. Solving the 1-dimensional linear movement of the displacement sensors from the 6-dimensional movement of the effector is called the forward solution; and solving the 6-dimensional movement of the effector from the 1-dimensional linear movement of the displacement sensors is called the inverse solution.

According to the principle of 6-point positioning [9], to solve the 6-dimensional movement of the effector through the inverse solution, it needs to arrange 6 displacement sensors around the target reference block. There are two types of the configuration of the 6 displacement sensors: 321-type and 222-type. The configuration of the displacement sensors of the 321-type ODM system is: 3 sensors are arranged in the first direction, 2 sensors are arranged in the second direction, and 1 sensor is arranged in the third direction; as for the 222-type ODM system, the configuration is to arrange 2 sensors in each direction of the three orthogonal directions.

2.2. Pose calculation method

FAN [10] et al. used the laser interferometer to measure the 6-dimensional parameters of the linear placement platform, and their pose calculation method is relatively simple: linear displacement is solved by using mean value method and the angular displacement is solved by using trigonometric functions. However, if the laser beam is not accurately aligned with the target object of the linear placement platform, such solving method is easy to introduce alignment errors. For example, if the axis of the target prism is not parallel with the axis of the laser beam, it'll generate Abbe error; if the axis of the target prism is not parallel with the axis of the laser beam, it'll generate axis error, etc. The expressions of each plane of the target reference block and the linear expressions of the displacement sensors in the measurement coordinate system could be obtained by using the three coordinates to measure the spatial positions of the target reference block and the displacement sensors; the target reference block could be solved using spatial analytical geometry method, and further, the pose of the moving platform could be obtained. In view of this, this study chooses to apply spatial analytical geometry method to solve the problem.

With a 222-type ODM system as an example, the inverse kinematics solution process is discussed as follows.

2.3. Forward kinematics solution

To facilitate the description of the relationship between the fixed platform reference system and the moving platform coordinate system of the fine-tuned mechanism, a coordinate system of the reference block {*E*} (hereinafter referred to as the reference block

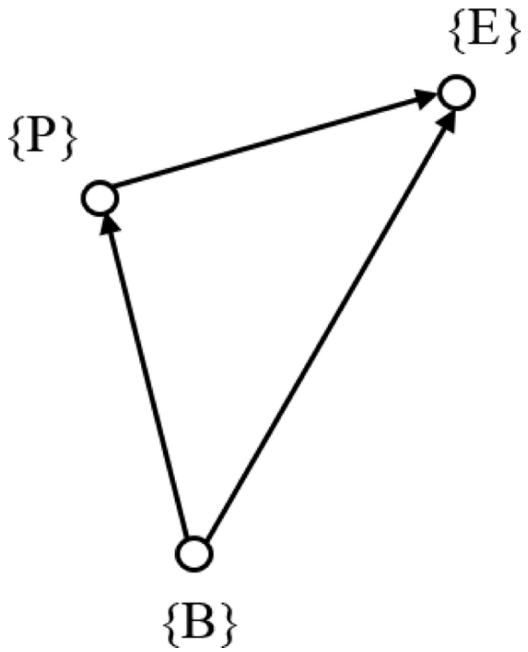

Fig. 2. Space dimension chain.

system) is constructed, the coordinate origin is located at the intersection of the three reference planes, and the coordinate axis is parallel to the moving platform coordinate system; as a result, in Fig. 2, there are following coordinate systems: the fixed platform reference system of the parallel mechanism {B}, the moving platform coordinate system of the parallel mechanism {P}, the coordinate system of the reference block {E}.

The pose relationship between the two systems is described by the corresponding homogeneous transformation matrix as:

${}^{B}_{P}T$ describes the pose of the moving platform coordinate system{P} relative to the fixed platform coordinate system {B};

${}^{P}_{E}T$ describes the pose of the reference block coordinate system {E} in the moving platform coordinate system{P}.

In order to intuitively describe the coordinate transformation, the above pose relationship can be expressed in the form of space dimension chain [11], as shown in Fig. 4.7.

The coordinate transformation equation is:

$$ {}^{B}_{E}T = {}^{B}_{P}T\,{}^{P}_{E}T \tag{1} $$

Assume that the pose of {E} in the moving platform coordinate system {P} is:

$$ {}^{P}_{E}Q = \begin{bmatrix} {}^{P}X_E & {}^{P}Y_E & {}^{P}Z_E & {}^{P}_{E}\alpha & {}^{P}_{E}\beta & {}^{P}_{E}\gamma \end{bmatrix} \tag{2} $$

Which can be written in the form of homogeneous coordinate transformation matrix [12], and abbreviated as:

$$ \begin{aligned} {}^{P}_{E}T &= \begin{bmatrix} c^{P}_{E}\beta c^{P}_{E}\gamma & c^{P}_{E}\gamma s^{P}_{E}\alpha s^{P}_{E}\beta - c^{P}_{E}\alpha s^{P}_{E}\gamma & c^{P}_{E}\alpha c^{P}_{E}\gamma s^{P}_{E}\beta + s^{P}_{E}\alpha s^{P}_{E}\gamma & {}^{P}X_E \\ c^{P}_{E}\beta s^{P}_{E}\gamma & s^{P}_{E}\alpha s^{P}_{E}\beta s^{P}_{E}\gamma + c^{P}_{E}\alpha c^{P}_{E}\gamma & c^{P}_{E}\alpha s^{P}_{E}\beta s^{P}_{E}\gamma - c^{P}_{E}\gamma s^{P}_{E}\alpha & {}^{P}Y_E \\ -s^{P}_{E}\beta & c^{P}_{E}\beta s^{P}_{E}\alpha & c^{P}_{E}\alpha c^{P}_{E}\beta & {}^{P}Z_E \\ 0 & 0 & 0 & 1 \end{bmatrix} \\ &= \begin{bmatrix} {}^{P}_{E}u_x & {}^{P}_{E}v_x & {}^{P}_{E}w_x & {}^{P}X_E \\ {}^{P}_{E}u_y & {}^{P}_{E}v_y & {}^{P}_{E}w_y & {}^{P}Y_E \\ {}^{P}_{E}u_z & {}^{P}_{E}v_z & {}^{P}_{E}w_z & {}^{P}Z_E \\ 0 & 0 & 0 & 1 \end{bmatrix} \end{aligned} \tag{3} $$

Where, c stands for cos, s stands for sin, same below.

Assume the actual pose of {E} in {B} at zero position is:

$$ {}^{B}_{E}Q^{(0)} = \begin{bmatrix} {}^{B}X_E & {}^{B}Y_E & {}^{B}Z_E & {}^{B}_{E}\alpha & {}^{B}_{E}\beta & {}^{B}_{E}\gamma \end{bmatrix} \tag{4} $$

Which can be written in the form of homogeneous coordinate transformation matrix, and abbreviated as:

$$ {}^{B}_{E}T^{(0)} = \begin{bmatrix} {}^{B}_{E}u_x & {}^{B}_{E}v_x & {}^{B}_{E}w_x & {}^{B}X_E \\ {}^{B}_{E}u_y & {}^{B}_{E}v_y & {}^{B}_{E}w_y & {}^{B}Y_E \\ {}^{B}_{E}u_z & {}^{B}_{E}v_z & {}^{B}_{E}w_z & {}^{B}Z_E \\ 0 & 0 & 0 & 1 \end{bmatrix} \tag{5} $$

Mark the XOY plane of coordinate system {E} as plane I, the XOZ plane as plane II, the YOZ plane as plane III, then the point normal equation of plane I can be obtained as [13]:

$$ {}^{B}_{E}w_x(x - {}^{B}X_E) + {}^{B}_{E}w_y(y - {}^{B}Y_E) + {}^{B}_{E}w_z(z - {}^{B}Z_E) = 0 \tag{6} $$

This expression is not conducive to programming and calculation, to facilitate programming, the expression of plane I is written as:

$$ I = \begin{bmatrix} x & y & z & dx_1 & dy_1 & dz_1 & dx_2 & dy_2 & dz_2 \end{bmatrix} \tag{7} $$

Where, $P = \begin{bmatrix} x_0 & y_0 & z_0 \end{bmatrix}$ represents the coordinates of a point on the plane, $v_1 = \begin{bmatrix} dx_1 & dy_1 & dz_1 \end{bmatrix}$ and $v_2 = \begin{bmatrix} dx_2 & dy_2 & dz_2 \end{bmatrix}$ represent vectors in the plane, and the direction of the plane normal vector n follows the right-hand rule.

The expressions of planes II and III are the same as that of plane I.

The parameter equation of the spatial straight line is [14]:

$$ \begin{cases} x = x_0 + mt \\ y = y_0 + nt \\ z = z_0 + pt \end{cases} \tag{8} $$

This expression is also not conducive to programming and calculation, so the expression of the spatial line of displacement sensor S_k is written as:

$$ L_k = \begin{bmatrix} x_k & y_k & z_k & dx_k & dy_k & dz_k \end{bmatrix}, k = 1, 2, 3, 4, 5, 6 \tag{9} $$

Where, $S_k = \begin{bmatrix} x_k & y_k & z_k \end{bmatrix}$ represents the coordinates of a point on the straight line, $v_k = \begin{bmatrix} dx_k & dy_k & dz_k \end{bmatrix}$ represents the straight line vector, $k = 1, 2, 3, 4, 5, 6$.

The linear equation and the plane equation of the displacement sensor are combined to obtain the coordinates of the contact points between each sensor and each coordinate plane when the moving platform is at zero position, which is recorded as:

$$M_k^{(0)} = \left[X_{Mk}^{(0)} \quad Y_{Mk}^{(0)} \quad Z_{Mk}^{(0)} \right], k = 1,2,3,4,5,6 \tag{10}$$

The pose of the moving platform is given and recorded as:

$$Q = [X_P \quad Y_P \quad Z_P \quad \alpha \quad \beta \quad \gamma] \tag{11}$$

Convert it into the form of homogeneous coordinate transformation matrix [15], then there is:

$${}_P^B T = \begin{bmatrix} c\beta c\gamma & c\gamma s\alpha s\beta - c\alpha s\gamma & c\alpha c\gamma s\beta + s\alpha s\gamma & X_P \\ c\beta s\gamma & s\alpha s\beta s\gamma + c\alpha c\gamma & c\alpha s\beta s\gamma - c\gamma s\alpha & Y_P \\ -s\beta & c\beta s\alpha & c\alpha c\beta & Z_P \\ 0 & 0 & 0 & 1 \end{bmatrix} \tag{12}$$

From Eqs. (3) and (12), the pose of coordinate system {E} in {B} can be obtained as:

$${}_E^B T = \begin{bmatrix} {}_E^B u_x & {}_E^B v_x & {}_E^B w_x & {}^B X_E \\ {}_E^B u_y & {}_E^B v_y & {}_E^B w_y & {}^B Y_E \\ {}_E^B u_z & {}_E^B v_z & {}_E^B w_z & {}^B Z_E \\ 0 & 0 & 0 & 1 \end{bmatrix} \tag{13}$$

So, the expressions of the three planes I, II, and III of {E} can be obtained and written as:

$$\begin{cases} I = \left[{}^B X_E \quad {}^B Y_E \quad {}^B Z_E \quad \cdots \quad {}_E^B v_x \quad {}_E^B v_y \quad {}_E^B v_y \right] \\ II = \left[{}^B X_E \quad {}^B Y_E \quad {}^B Z_E \quad \cdots \quad {}_E^B u_x \quad {}_E^B u_y \quad {}_E^B u_z \right] \\ III = \left[{}^B X_E \quad {}^B Y_E \quad {}^B Z_E \quad \cdots \quad {}_E^B w_x \quad {}_E^B w_y \quad {}_E^B w_z \right] \end{cases} \tag{14}$$

By combining the linear equation and the plane equation of the displacement sensors, the contact point coordinates of each sensor and each coordinate plane can be obtained as:

$$M_k^{(1)} = \left[X_{Mk}^{(1)} \quad Y_{Mk}^{(1)} \quad Z_{Mk}^{(1)} \right], k = 1,2,3,4,5,6 \tag{15}$$

From Eqs. (10) and (15), the linear distance between the two contact points can be obtained as:

$$|h_k| = \sqrt{\left(X_{Mk}^{(1)} - X_{Mk}^{(0)}\right)^2 + \left(Y_{Mk}^{(1)} - Y_{Mk}^{(0)}\right)^2 + \left(Z_{Mk}^{(1)} - Z_{Mk}^{(0)}\right)^2} \tag{16}$$

If the contact point moves in the positive direction of the coordinate axis, it's specified that h is positive, otherwise it is negative, namely:

$$\begin{cases} h_k = |h_k|, h_k \geq 0 \\ h_k = -|h_k|, h_k < 0 \end{cases} \tag{17}$$

Write the displacement of each displacement sensor into the vector form, then there is:

$$H = [h_1 \quad h_2 \quad h_3 \quad h_4 \quad h_5 \quad h_6] \tag{18}$$

Therefore, from the pose of the moving platform, the placement value of each placement sensor could be obtained, namely the forward kinematics solutions.

2.4. Inverse kinematics solution

Assume after the pose has changed, the stretching-and-drawing amount of each displacement sensor is $h_k, k = 1,2,3,4,5,6$.

At this time, the contact points between displacement sensors and planes I, II, and III would change accordingly, the coordinates M^k in {B} are:

$$\begin{cases} X_{Mk}^{(1)} = X_{Mk}^{(0)} + h_k * dx_k \Big/ \sqrt{dx_k^2 + dy_k^2 + dz_k^2} \\ Y_{Mk}^{(1)} = Y_{Mk}^{(0)} + h_k * dy_k \Big/ \sqrt{dx_k^2 + dy_k^2 + dz_k^2} \\ Z_{Mk}^{(1)} = Z_{Mk}^{(0)} + h_k * dz_k \Big/ \sqrt{dx_k^2 + dy_k^2 + dz_k^2} \end{cases} \tag{19}$$

Assume the normal vector of plane I is $[{}_E^M w_x \quad {}_E^M w_y \quad {}_E^M w_z]$, the normal vector of plane II is $[{}_E^M v_x \quad {}_E^M v_y \quad {}_E^M v_z]$, the normal vector of plane III is $[{}_E^M u_x \quad {}_E^M u_y \quad {}_E^M u_z]$, the three normal vectors are perpendicular to the vectors in each plane, then there is [16]:

$$\begin{cases} w_x * (X_{M2} - X_{M1}) + w_y * (Y_{M2} - Y_{M1}) + w_z * (Z_{M2} - Z_{M1}) = 0 \\ v_x * (X_{M4} - X_{M3}) + v_y * (Y_{M4} - Y_{M3}) + v_z * (Z_{M4} - Z_{M3}) = 0 \\ u_x * (X_{M6} - X_{M5}) + u_y * (Y_{M6} - Y_{M5}) + u_z * (Z_{M6} - Z_{M5}) = 0 \end{cases} \tag{20}$$

The three-plane normal vectors are perpendicular to each other, so there is:

$$\begin{cases} w_x{}^*u_x + w_y{}^*u_y + w_z{}^*u_z = 0 \\ w_x{}^*v_x + w_y{}^*v_y + w_z{}^*v_z = 0 \\ v_x{}^*u_x + v_y{}^*u_y + v_z{}^*u_z = 0 \end{cases} \tag{21}$$

Also, the unit vector modulus is 1, there is:

$$\begin{cases} {}^M_E w_x^2 + {}^M_E w_y^2 + {}^M_E w_z^2 = 1 \\ {}^M_E v_x^2 + {}^M_E v_y^2 + {}^M_E v_z^2 = 1 \\ {}^M_E u_x^2 + {}^M_E u_y^2 + {}^M_E u_z^2 = 1 \end{cases} \tag{22}$$

There are 9 unknown quantities and 9 equations, so the unknowns can be calculated, therefore, the programming expressions of planes I, II and III can be written as:

$$\begin{cases} I = \begin{bmatrix} X_{M1} & Y_{M1} & Z_{M1} & \cdots & {}^M_E v_x & {}^M_E v_y & {}^M_E v_z \end{bmatrix} \\ II = \begin{bmatrix} X_{M1} & Y_{M1} & Z_{M1} & \cdots & {}^M_E w_x & {}^M_E w_y & {}^M_E w_z \end{bmatrix} \\ III = \begin{bmatrix} X_{M1} & Y_{M1} & Z_{M1} & \cdots & {}^M_E w_x & {}^M_E w_y & {}^M_E w_z \end{bmatrix} \end{cases} \tag{23}$$

The expressions of the three planes are combined to obtain the intersection point of the three planes, which is recorded as:

$${}^M E = \begin{bmatrix} {}^M X_E & {}^M Y_E & {}^M Z_E \end{bmatrix} \tag{24}$$

So, the homogeneous coordinate transformation matrix of $\{E\}$ in $\{M\}$ can be obtained as:

$${}^M_E T = \begin{bmatrix} {}^M_E u_x & {}^M_E v_x & {}^M_E w_x & {}^M X_E \\ {}^M_E u_y & {}^M_E v_y & {}^M_E w_y & {}^M Y_E \\ {}^M_E u_z & {}^M_E v_z & {}^M_E w_z & {}^M Z_E \\ 0 & 0 & 0 & 1 \end{bmatrix} \tag{25}$$

From Eq. (1), it's known that:

$${}^B_P T = \left({}^M_B T\right)^{-1} {}^M_E T \left({}^P_E T\right)^{-1} \tag{26}$$

Which is abbreviated as

$${}^B_P T = \begin{bmatrix} {}^B_P u_x & {}^B_P v_x & {}^B_P w_x & {}^B X_P \\ {}^B_P u_y & {}^B_P v_y & {}^B_P w_y & {}^B Y_P \\ {}^B_P u & {}^B_P v_z & {}^B_P w_z & {}^B Z_P \\ 0 & 0 & 0 & 1 \end{bmatrix}_y \tag{27}$$

According to the RPY inverse solution equation [11], there is:

$$\begin{cases} \alpha = \arctan\left(\dfrac{{}^B_P v_z}{{}^B_P w_z}\right) \\ \beta = \arctan\left(\dfrac{-{}^B_P u_z}{\sqrt{{}^B_P u_x^2 + {}^B_P v_y^2}}\right) \\ \gamma = \arctan\left(\dfrac{{}^B_P u_y}{{}^B_P u_x}\right) \end{cases} \tag{28}$$

As a result, the pose of the moving platform coordinate system in the fixed platform coordinate system has been solved to be:

$$Q = \begin{bmatrix} {}^B X_P & {}^B Y_P & {}^B Z_P & \alpha & \beta & \gamma \end{bmatrix} \tag{29}$$

Which is the inverse kinematics solution of the ODM system.

From the solution process of the pose, it can be seen that, although the whole process seems a bit complex, its requirement on data amount is less, and it is easy to operate, which are the advantages of this method.

3. The error model based on the infinitesimal displacement synthesis method

Each time the moving platform changes a pose, a constraint equation can be constructed for each displacement sensor, so it's assumed:

$$h^{jk} = f(X_{Bi}, Y_{Bi}, Z_{Bi}, X_{Pi}, Y_{Pi}, Z_{Pi}, l_i, x_k, y_k, z_k, dx_k, dy_k, dz_k)$$
$$i = 1,2,3,4,5,6, k = 1,2,3,4,5,6 \tag{30}$$

Where, $X_{Bi}, Y_{Bi}, Z_{Bi}, X_{Pi}, Y_{Pi}, Z_{Pi}, l_i$ are the structural parameters of the parallel mechanism, and $x_k, y_k, z_k, dx_k, dy_k, dz_k$ are the structural parameters of the ODM system.

When there're errors in the structural parameters, the equation becomes:

$$h_{jk} + \Delta h_{jk} = f(X_{Bi} + \Delta X_{Bi}, ..., l_i + \Delta l_i, x_k + \Delta x_k, \cdots, dz_6 + \Delta dz_6) \tag{31}$$

Where, j = 1,2,3,… represents different positions and postures, so there is:

$$\Delta h_{jk} = f(X_{Bi} + \Delta X_{Bi}, ..., l_i + \Delta l_i, x_k + \Delta x_k, \cdots, dz_6 + \Delta dz_6) - h_{jk} \tag{32}$$

Where, $\Delta X_{Bi}, ..., \Delta l_i, \Delta x_k, \cdots, \Delta dz_6$ are the structural parameter errors of the parallel mechanism and the ODM system, Δh_{jk} is the deviation in the indicating values of the displacement sensors caused by the structural parameter errors.

Therefore, an error model of the combination of the parallel mechanism and the ODM system has been constructed based on the infinitesimal displacement synthesis method, in the model, Δh_{jk} can be obtained from the difference between the measured value and the nominal value of the displacement sensor, $X_{Bi}, Y_{Bi}, Z_{Bi}, X_{Pi}, Y_{Pi}, Z_{Pi}, l_i, x_k, y_k, z_k, dx_k, dy_k, dz_k$ are the nominal values of the parameters of the parallel mechanism and the ODM system, and they are known quantities; $\Delta X_{Bi}, \cdots, \Delta l_i, \Delta x_k, \cdots, \Delta dz_k$ are unknown quantities, each structural parameter error can be obtained by solving the above equation.

4. Parameter error identification based on optimization algorithm

4.1. Construction of the parameter error identification model

After obtaining the test data, how to obtain reasonable kinematics parameter error identification results is the difficulty and the key point of the entire kinematics calibration. Adopting different methods to process the test data can yield different parameter identification results. According to the identification model, parameter error identification methods can be divided into two categories: one is the error identification method based on the linear error model [17–19], which establishes the function mapping relationship between structural parameter errors and error measurement results by identifying the Jacobian matrix, and then identifies the structural parameters by solving this model, it can be summarized as the solution of typical linear equations; in the actual application process, it requires the parallel mechanism move along a fixed trajectory, its flexibility is low and the computation workload is large. The other is the error identification method based on the optimization algorithm, this method does not establish a linear error model, but uses the optimization algorithm to directly search for the kinematics parameter errors. Methods of this kind are based on the machine kinematics equations and error measurement results, there's no specific identification equation, they are a kind of typical non-linear equation solution, and the commonly used solving methods include genetic algorithm [20], neural network [21] and so on.

The error model proposed in the paper is non-linear, it is impossible to construct a linear equation set to solve the errors of the structural parameters, so we can only choose the second method.

The parameter error identification problem of the above model can be converted into an optimization problem of the minimization of objective function. The mathematical model of the optimization problem is constructed as follows:

Under each pose, taking the minimum sum of squares of the indicating value errors of the displacement sensor as the objective function, that is:

$$\sum_{j=1}^{m} \sum_{k=1}^{6} \left(\Delta h_{jk}\right)^2 = \min \tag{33}$$

Taking the structural parameter errors of the parallel mechanism and the calibration device as the design variables, namely:

$$X = [\Delta X_{B1} \quad \cdots \quad \Delta Z_{P6} \quad \Delta x_1 \quad \cdots \quad \Delta dz_6]_{1\times 78} \tag{34}$$

The constraint condition of each variable is the value range of the variable under the condition of existing processing and assembly capabilities, it takes ±0.2 (mm/rad).

4.2. Selection of the optimization tool

The identification of structural parameter errors is to search for the solutions that satisfy Eq. (33) within the value range of the design variables. The simplest random search can be used to complete this work, but random search has slow computation speed and large computation load. Common optimization algorithms such as genetic algorithm have the characteristics of global search, stable and reliable, and there's no need to solve the equation; however, these algorithms generally have large computation workload, long computation time, they cannot handle the expensive constraints, and are easy to fall into local optimal solutions. On this occasion, the new-generation intelligent optimization design software OASIS has provided an effective way to solve the above questions. The full name of OASIS is Optimization Assisted System Integration Software, OASIS has integrated leading AI algorithms in the industry, can automatically run the simulation software, change the input files, and restart the design process, thereby eliminating the bottleneck in

the traditional development design process, making the entire design process achieve full digitalization and automation, and ultimately solving a series of the design optimization problems more rapidly and efficiently [22,23].

In summary, this paper attempts to apply this software to the parameter error identification.

5. Parameter calibration test of the parallel mechanism

To verify the effectiveness of the above method, a parameter calibration test was performed on the parallel mechanism.

5.1. Calibration objects and test elements

In this paper, the object of parameter calibration is a set of 6-DOF 6-SPS parallel mechanisms, as shown in Fig. 3. Its structural parameters are shown in Table 1. The calibration test elements include 6 displacement sensors, sensor stand, and reference block to be measured (target reference block), etc., as shown in Fig. 4. The displacement sensors are SM30 series Czech ESSA grating displacement sensors, which have the advantages of large measurement range, high resolution and high accuracy, etc. [24].

5.2. Calibration test process

Based on the 222-type ODM system, the calibration test was carried out, and the photo of the test site is shown in Fig. 5. The displacement sensors S1 and S2 were located in the + Z direction of the target reference block, S3 and S4 were located in the -Y direction, and S5 and S6 were located in the -X direction. The monitor 1 shows the data of S1, S2, and S3; and monitor 2 shows the data of S4, S4, and S6.

Measurement configuration consisted of 18 positions and postures was selected, as shown in Table 2; the corresponding theoretical values of the 18 displacement sensors are shown in Table 3; displacement measurement was conducted, and the indicating values of the displacement sensors are shown in Table 4.

According to the above data, an OASIS-based optimization model was constructed, the variables are the structural parameter errors of the parallel mechanism and the ODM system, the value range is ±0.2 (mm/rad) and the step size is 0.001 (mm/rad). The objective function is the minimum sum of squares of the sensors' indicating value errors under each pose. The optimization calculation was carried out in OASIS, the process is shown in Fig. 6, and the calculation process is shown in Fig. 7. After more than 200 rounds of iterations, the structural parameter errors of the parallel mechanism and the ODM system were obtained, and then the compensated structural parameters were obtained as well. The structural parameters of the parallel mechanism after compensation are shown in Table 5.

The parameters in the control program of the parallel mechanism were modified, then the positions and postures of the calibration test were input respectively to make the moving platform move to the specified pose, so as to verify the calibration effect. After that, the structural parameters of the ODM system before and after the compensation, and the indicating values of the displacement sensors were substituted into the inverse kinematics solutions of the ODM system to obtain the errors of the pose before and after the compensation, as shown in Fig. 8.

According to the figure, there are:

1) For ΔX_P, the maximum error was about 0.171 mm before calibration and about 0.01 mm after calibration, which was reduced by about 94 %;

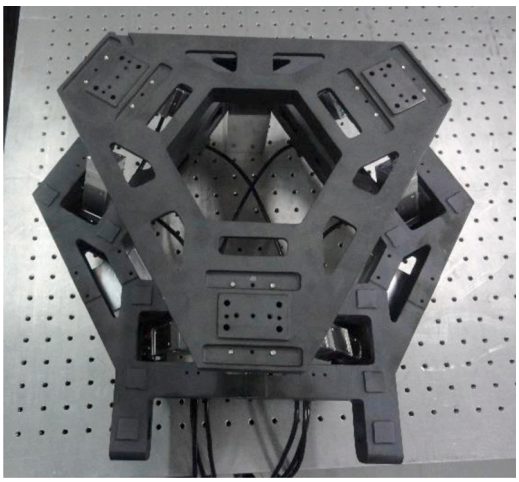

Fig. 3. 6-DOF parallel mechanism.

Fig. 4. SM30 series ESSA grating displacement sensor.

Table 1
Nominal value of 42 kinematic parameters of 6-SPS parallel mechanism(Unit: mm).

Branch	X_{Bi}	Y_{Bi}	Z_{Bi}	X_{Pi}	Y_{Pi}	Z_{Pi}	l_i
1	−138	99.354	0	−138	17.965	0	141.898
2	−138	−99.354	0	−138	−17.965	0	141.898
3	−17.043	−169.189	0	53.442	−128.494	0	141.898
4	155.043	−69.834	0	84.558	−110.529	0	141.898
5	155.043	69.834	0	84.558	110.529	0	141.898
6	−17.043	169.189	0	53.442	128.494	0	141.898

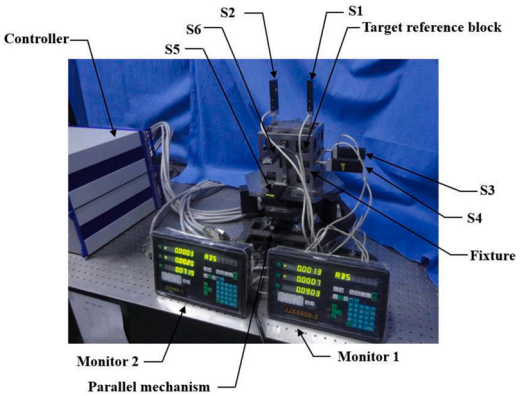

Fig. 5. Data collection site of 222-type ODM system.

2) For ΔY_P, the maximum error was about 0.073 mm before calibration and about 0.01 mm after calibration, which was reduced by about 87 %;
3) For ΔZ_P, the maximum error was about 0.032 mm before calibration and about 0.01 mm after calibration, which was reduced by about 69 %;
4) For $\Delta\alpha$, the maximum error was about 1.3×10^{-5} rad before calibration and about 1.7×10^{-6}rad after calibration, which was reduced by about 87 %;
5) For $\Delta\beta$, the maximum error was about 6.7×10^{-4} rad before calibration and about 1.7×10^{-5}ad after calibration, which was reduced by about 97 %;
6) For $\Delta\gamma$, the maximum error was about 2.3×10^{-4} rad before calibration and about 1.7×10^{-5}rad after calibration, which was reduced by about 93 %.

In summary, the pose errors after calibration were significantly lower than those before calibration, indicating that the calibration effect is significant.

Compared with the traditional measuring devices and methods, the pose measuring device and method proposed in this paper have the following advantages:

Table 2
Measurement configurations of calibration experiment (unit: mm/rad).

No.	X	Y	Z	α	β	γ
1	3.94	−5.85	116.69	−0.010	0.012	−0.001
2	3.94	6.07	116.30	0.019	−0.016	0.003
3	3.94	−0.25	116.71	0.004	0.008	0.000
4	−5.17	−5.85	116.69	0.019	−0.016	0.000
5	−5.17	6.07	116.30	0.004	0.008	−0.001
6	−5.17	−0.25	116.71	−0.010	0.012	0.003
7	0.20	−5.85	116.30	−0.010	0.008	0.003
8	0.20	6.07	116.71	0.019	0.012	0.000
9	0.20	−0.25	116.69	0.004	−0.016	−0.001
10	3.94	−5.85	116.71	0.004	−0.016	0.003
11	3.94	6.07	116.69	−0.010	0.008	0.000
12	3.94	−0.25	116.30	0.019	0.012	−0.001
13	−5.17	−5.85	116.30	0.004	0.012	0.000
14	−5.17	6.07	116.71	−0.010	−0.016	−0.001
15	−5.17	−0.25	116.69	0.019	0.008	0.003
16	0.20	−5.85	116.71	0.019	0.008	−0.001
17	0.20	6.07	116.69	0.004	0.012	0.003
18	0.20	−0.25	116.30	−0.010	−0.016	0.000

Table 3
Nominal value of displacement sensor of calibration experiment (unit: mm).

No.	h1	h2	h3	h4	h5	h6
1	−0.2403	0.552	1.789	−4.2485	−4.1919	6.4976
2	0.9121	0.111	−2.1186	3.3031	2.9095	0.4466
3	0.0513	1.1968	0.7527	−0.8175	−0.8526	5.6124
4	1.6729	0.8633	−1.3612	−8.7478	−8.822	−8.6712
5	−0.4558	0.6897	0.2448	5.4391	5.5136	−3.4925
6	−0.2644	0.5209	1.763	1.5796	1.2071	−2.6117
7	−0.4399	−0.1406	1.1	−4.0351	−4.4026	1.8607
8	−0.2857	2.2367	0.0134	3.1333	3.1208	2.7586
9	1.4412	−0.2599	−0.7032	−0.8658	−0.8018	−3.3019
10	1.4245	−0.2716	−0.7218	−6.2635	−6.6286	0.4177
11	0.1013	0.4051	1.6433	7.7154	7.6673	5.6146
12	−0.5377	1.9833	−0.2413	−3.2411	−3.1438	6.4988
13	−0.667	0.9652	0.5212	−6.4172	−6.4506	−2.6076
14	1.6221	−0.9192	0.3199	7.6431	7.7341	−8.6726
15	−0.0028	2.0376	−0.1833	−3.0036	−3.3445	−3.4929
16	0.1694	2.2035	−0.0207	−8.832	−8.7437	1.8787
17	−0.2573	1.3741	0.9339	5.6565	5.3038	2.7747
18	1.0576	−1.4839	−0.2466	1.3912	1.3724	−3.3084

Table 4
Measurement value of displacement sensor of calibration experiment (unit: mm).

No.	h1	h2	h3	h4	h5	h6
1	−0.2641	0.7010	1.8504	−4.2890	−4.2548	6.5308
2	0.9735	−0.1198	−2.2568	3.3596	2.9603	0.4045
3	0.1050	1.2667	0.7146	−0.8101	−0.8554	5.6342
4	1.7750	0.7031	−1.4550	−8.8325	−8.9709	−8.6974
5	a−0.4042	0.7718	0.2172	5.4853	5.6018	−3.4733
6	−0.2846	0.6921	1.8397	1.5483	1.1900	−2.5875
7	−0.4787	−0.0279	1.1715	−4.0990	−4.4941	1.8761
8	−0.1171	2.3213	−0.1328	3.1921	3.1924	2.7933
9	1.4219	−0.4294	−0.7102	−0.8661	−0.8111	−3.3383
10	1.4085	−0.4445	−0.7324	−6.3197	−6.7417	0.3735
11	0.0469	0.4937	1.6965	7.7832	7.7863	5.6332
12	−0.3687	2.0590	−0.3937	−3.2350	−3.1668	6.5369
13	−0.5831	1.1106	0.5034	−6.4942	−6.5635	−2.5760
14	1.5065	−1.0508	0.4192	7.6888	7.8388	−8.7077
15	0.1693	2.1124	−0.3059	−3.0378	−3.4079	−3.4724
16	0.3434	2.2705	−0.1486	−8.8972	−8.8707	1.9054
17	−0.1941	1.4882	0.8947	5.7033	5.3779	2.8024
18	0.9348	−1.6364	−0.1569	1.3901	1.3815	−3.3492

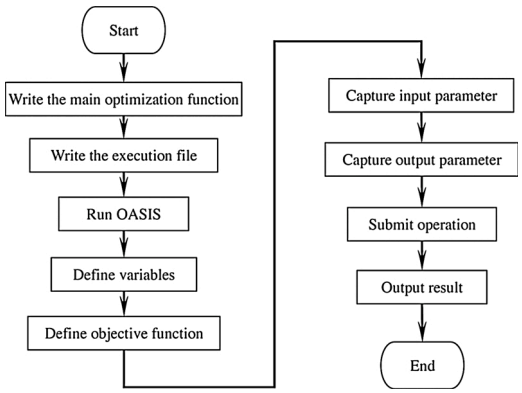

Fig. 6. Flow of optimization.

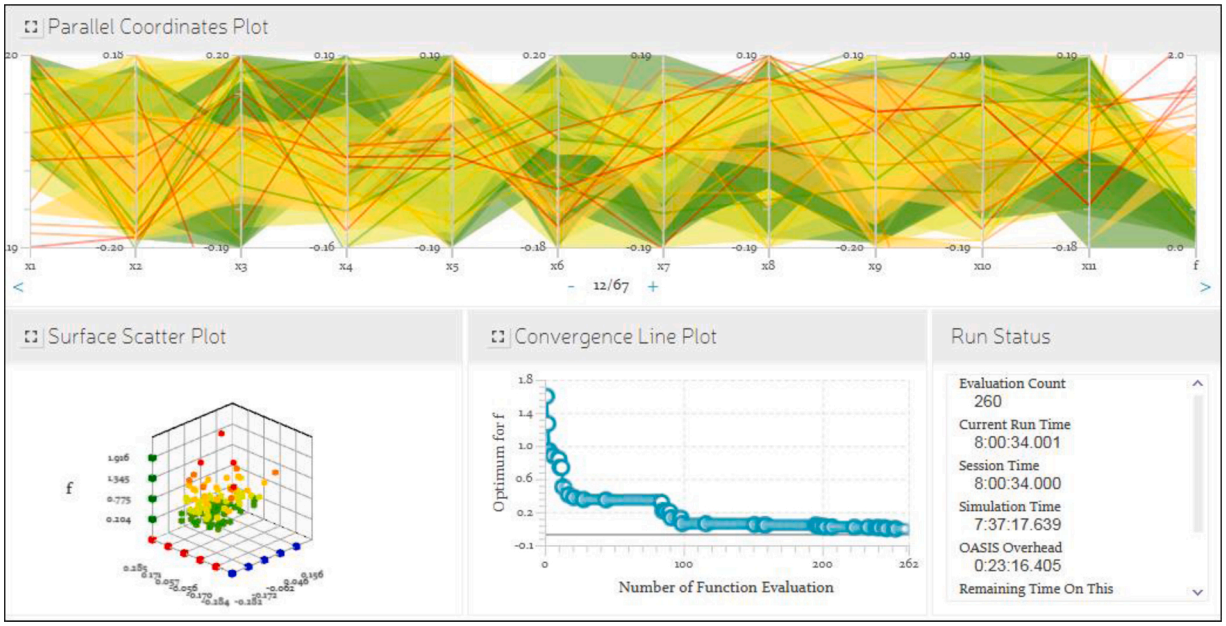

Fig. 7. OASIS visualization calculation process.

Table 5
42 kinematic parameters after compensation (unit: mm).

Branch	X_{Bi}	Y_{Bi}	Z_{Bi}	X_{Pi}	Y_{Pi}	Z_{Pi}	l_i
1	−137.991	99.282	−0.070	−138.048	18.033	−0.049	141.860
2	−137.937	−99.406	0.086	−138.030	−18.026	−0.050	141.904
3	−17.020	−169.194	−0.030	53.508	−128.477	0.010	141.831
4	155.127	−69.877	0.051	84.609	−110.553	0.014	141.918
5	154.959	69.745	0.006	84.614	110.616	−0.074	141.851
6	−17.030	169.183	−0.098	53.409	128.426	0.059	141.929

1) Easy to operate. To measure pose, the proposed device and method only need to fix the target reference block on the moving platform of the parallel mechanism and fix the displacement sensors on the stand.
2) Simple and efficient. As long as the end pose of the parallel mechanism change, the indicating values of the displacement sensors would change accordingly, by substituting them into the inverse kinematics solutions, the end pose information could be obtained, which can greatly save the labor and time costs.
3) Low cost. The main components of the measuring system are: 6 high-precision displacement sensors (reusable), target reference block and measuring reference block, and stand for the sensors, so, the overall cost is relatively low.

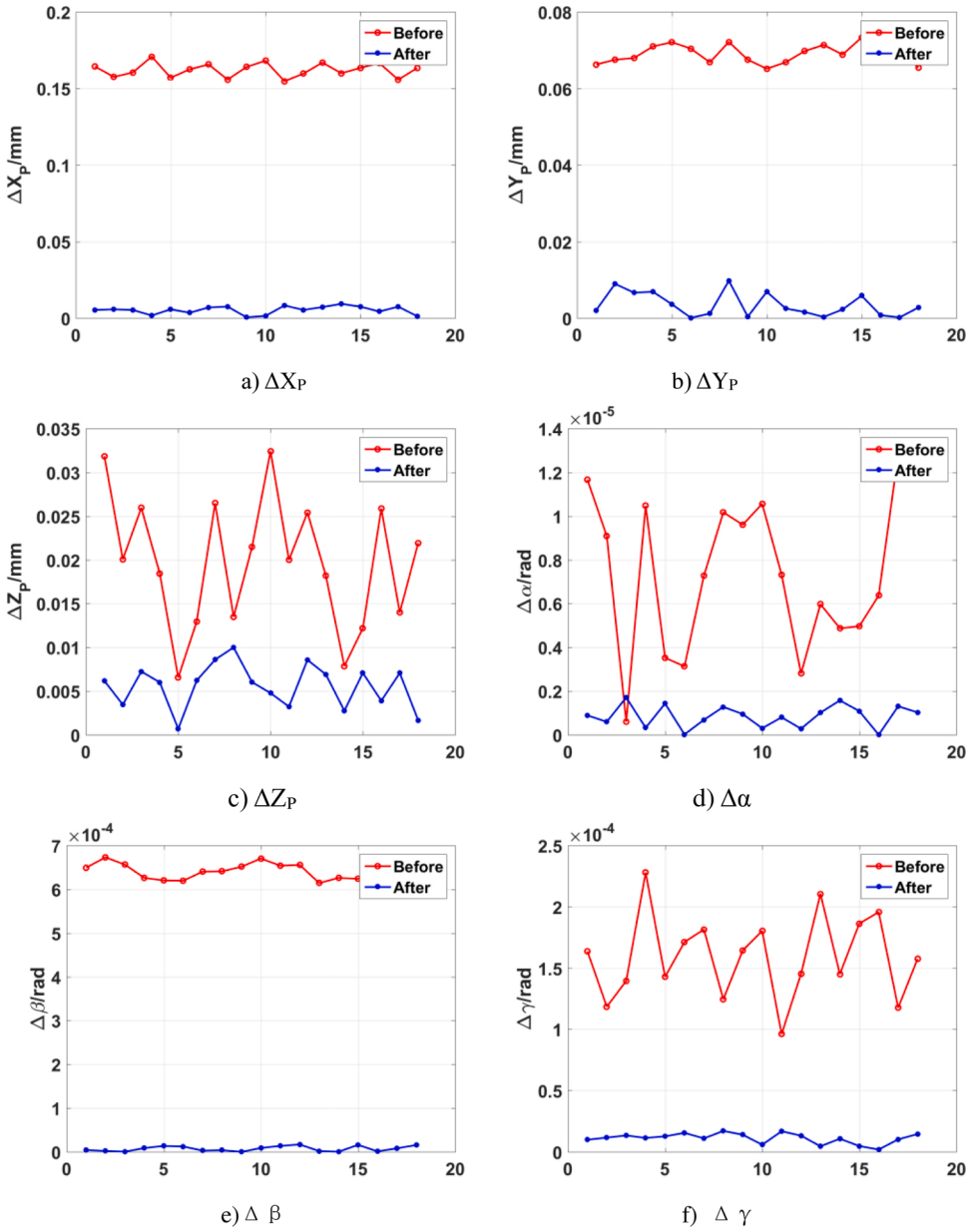

Fig. 8. Pose errors before and after calibration.

In summary, the pose measuring device and method proposed in this paper can not only effectively improve the positioning accuracy of the parallel mechanism, but also have the advantages of easy-to-operate, simple and efficient, and low cost.

6. Conclusion

To simplify the parameter calibration process of the 6-DOF parallel mechanism, improve the calibration efficiency, and reduce the calibration cost, this paper proposed a pose measuring method based on the ODM system, applied the spatial analytic geometry method to analyze the forward and inverse kinematics solutions of the ODM system, and adopted the infinitesimal displacement synthesis method to construct an error model for the combination of the parallel mechanism and the ODM system. Then, to identify the structural parameters of the parallel mechanism, a mathematical model of the optimization problem was constructed, and the objective function was the minimum sum of squares of the sensors' indicating value errors, and the design variables were the structural parameter errors of the parallel mechanism and the calibration device. After that, a parallel mechanism calibration platform based on the ODM system was constructed, and the displacement of the 6-DOF parallel mechanism was measured; the OASIS software was used to identify the structural parameter errors of the parallel mechanism and compensate the structural parameters, and then the effect of

the compensation was verified. The comparison of the pose errors before and after calibration showed that the maximum position error was reduced by 69 %–94 %, and the maximum posture error was reduced by 87 %–97 %, indicating that the positioning accuracy of the parallel mechanism had been improved effectively. Compared with the traditional calibration method, the proposed method has the advantages of easy-to-operate, simple and efficient, and low cost; it can effectively simplify the calibration work, improve the calibration efficiency, and reduce the calibration cost.

The research results of this paper have high guiding significance and reference value for the calibration of parallel mechanisms.

Declaration of Competing Interest

We declare that we have no financial and personal relationships with other people or organizations that can inappropriately influence our work in the manuscript *Parameter Calibration of 6-Degree-of-Freedom Parallel Mechanism Based on Orthogonal Displacement Measuring System*.

Acknowledgement

The author(s) disclosed receipt of the following financial support for the research and/or authorship of this article: This work is supported by the National Key Research and Development Program (No.2016YFB0500100), the Civil Aerospace Pre-research Project (No.D040101), and the National Natural Science Foundation of China(NO.11873007).

References

[1] C.Y. Han, Z.B. Xu, Q.W. Wu, et al., Optimization design and error distribution for secondary mirror adjusting mechanism of large optical payload, Opt. Precis. Eng. 24 (5) (2016) 1094–1103.
[2] R. Fan, X. Li, D. Wang, Integral Kinematic Calibration of 6UPS Parallel Mechanism, J. Beijing Univ. Aeronaut. Astronaut. 42 (5) (2016) 871–877.
[3] L.Y. Li, Method Studies on Error Modeling and Calibration of the Stewart Platform, Yanshan University, Q zinghuangdao, 2006.
[4] H. Yan, J.F. He, Q.T. Huang, et al., Calibration of Stewart Platforms Using a Coordinate Measuring Machine, Mach. Tool Hydrauics 35 (7) (2007) 11–14.
[5] D.Y. Yu, Accuracy Analysis and Calibration of Six-DOF Motion Simulator, Harbin Institute of Technology, Harbin, 2006.
[6] Z.Y. Geng, Error Analysis and Calibration of the Position and Attitude of the Stewart Platform, Xi'an University of Electronic Science and Technology, Xi'an, 2014.
[7] Q.X. Li, A Construction of the Six-DOF Calibration System of Nanopositioning Stage Based on Laser Interferometer, Zhejiang Sci-Tech University, Hangzhou, 2014.
[8] C.F. Kuang, Q.B. Feng, B. Zhang, et al., Mathematic Model of Simultaneously Measuring Six-dimensional Parameters by Laser, Chin. J. Scientific Instrum. 27 (4) (2006) 348–352.
[9] F.Y. Li, Design of Universal Fixture for Industrial Robot Based on Six Point Positioning Theory, Machinery 44 (6) (2017) 77–80.
[10] K.C. Fan, M.J. Chen, W.M. Huang, A six-degree-of-Freedom measurement system for the motion accuracy of linear stages, Int. J. Mach. Tools Manuf. 38 (3) (1998) 155–164.
[11] Y.L. Xiong, W.L. Li, W.B. Chen, et al., Robotics: Modeling, Controlling and Visualization, Huazhong University of Science and Technology Press, Wuhan, 2018, p. 48.
[12] Y.L. Xiong, W.L. Li, W.B. Chen, et al., Robotics: Modeling, Controlling and Visualization, Huazhong University of Science and Technology Press, Wuhan, 2018, p. 40.
[13] Department of Mathematics, Tongji University. Advanced Mathematics Vol. (1) (4th Edition), Higher Education Press, Beijing, 1996, pp. 418–419.
[14] Department of Mathematics, Tongji University. Advanced Mathematics vol. (1) (4th Edition), Higher Education Press, Beijing, 1996, p. 426.
[15] G.Q. Zhang, J.J. Du, Calibration Test and Precision Analysis of Small Sized Hexapod Parallel Manipulator with High Accuracy, Nanotechnol. Precis. Eng. 11 (1) (2012) 34–40.
[16] Department of Mathematics, Tongji University. Advanced Mathematics Vol. (1) (4th Edition), Higher Education Press, Beijing, 1996, pp. 397–399.
[17] K. Wang, Research on Calibration and Error Compensation of Kinematics Parameters of Industrial Robots, Huazhong University of Science and Technology Press, Wuhan, 2018.
[18] L.Y. Kong, Kinematic Error Modeling and Parameter Identifiability Analysis of Parallel Mechanisms, Shanghai Jiao Tong University, Shanghai, 2018.
[19] D. Liu H, On the Measuring and Calibration for the Fine Tuning Stewart Platform of the Large Radio Telescope, Xi'an University of Electronic Science and Technology, Xi'an, 2008.
[20] W.T. He, Y.K. Tang, L.G. Zhang, et al., Robotic Kinematics Error Calibration Based on Genetic Algorithm, Mech. Sci. Technol. Aerosp. Eng. 34 (11) (2015) 1794–1799.
[21] H.Y. Liu, C.G. Yu, C. Zhao, Kinematics Calibration of Parallel Automatic Filling Robot, Ordnance Ind. Autom. 38 (6) (2019) 81–86.
[22] https://max.book118.com/html/2019/0717/5004302224002104.shtm [EB/OL].
[23] https://www.empowerops.cn/ai算法优势[EB/OL].
[24] http://www.jjx88.com/Upload/ProPdf/ESSA高分辨率光栅尺%20%20%20SM30.pdf[DB/OL].